The Effects of Radiation on 1/f Noise in Complementary (*npn* + *pnp*) SiGe HBTs

Enhai Zhao,*Student Member, IEEE*, Akil K. Sutton, *Student Member, IEEE*, Becca M. Haugerud, *Student Member, IEEE*, John D. Cressler, *Fellow, IEEE*, Paul W. Marshall, *Member, IEEE*, Robert A. Reed, *Member, IEEE*, Badih El-Kareh, *Member, IEEE*, Scott Balster *Member, IEEE*, and Hiroshi Yasuda, *Student Member, IEEE*

Abstract— **We present the first study of the effects of radiation on low-frequency noise in a complementary (*npn* + *pnp*) SiGe HBT BiCMOS technology. In order to manipulate the physical noise sources in these complementary SiGe HBTs, 63.3 MeV protons were used to generate additional (potentially noise-sensitive) traps states. The base currents of both the *npn* and *pnp* SiGe HBTs degrade with increasing proton fluence, as expected, although in general more strongly for the *npn* transistors than for the *pnp* transistors, particularly in inverse mode. For the *pnp* SiGe HBTs, irradiation has almost no effect on the 1/f noise to proton fluences as high as 5.0×10^{13} p/cm^2, while the *npn* SiGe HBTs show substantial radiation-induced excess noise. In addition, unlike for the *pnp* devices, which maintain an I_B^2 bias dependence, the 1/f noise of the post-irradiated *npn* SiGe HBTs change to a near-linear dependence on I_B at low base currents following radiation, suggesting a fundamental difference in the noise physics between the two types of devices.**

I. Introduction

High-speed complementary (*npn*+*pnp*) bipolar transistor technology has long been recognized for its many advantages in high-performance analog IC design, particularly for low voltage circuits and push-pull architectures. In such complementary technologies, however, maintaining adequate performance in the *pnp* transistor is very difficult, partially compromising the utility of complementary analog technologies. It is generally recognized that bandgap engineering using silicon-germanium (SiGe) alloys has a very favorable impact on key analog figures-of-merit such as gain, frequency response, output conductance, βV_A product, and noise [1], and many such SiGe HBT technologies are in wide-spread use today. Exclusively, however, such SiGe technologies are based around *npn* SiGe HBT configurations. *pnp* SiGe HBTs are known to be more challenging in their design and optimization [1], and the successful monolithic integration of SiGe *npn*'s and SiGe *pnp*'s to form a complementary SiGe analog technology has proven challenging to achieve. Recently, however, a novel complementary SiGe HBT BiCMOS technology on SOI has in fact been reported [2], opening the way to a new level of performance in analog IC design.

This work was supported by Texas Instruments, the Georgia Tech Analog Consortium, DTRA, NASA-GSFC, and the Georgia Electronic Design Center at Georgia Tech.

E. Zhao, A.K. Sutton, B.M. Haugerud and J.D. Cressler are with the School of Electrical and Computer Engineering, 85 Fifth Street, N.W., Georgia Institute of Technology, Atlanta, GA 30308, USA.
Tel:(404)894-5161/Fax:(404)894-4641/E-mail:zealing@ece.gatech.edu

P.W. Marshall is a consultant to NASA-GSFC.

R.A. Reed is with NASA-GSFC, Greenbelt, MD 20771 USA.

B. El-Kareh, S. Balster and H. Yasuda are with Texas Instruments, Freising, Germany.

Low-frequency noise in transistors usually exhibits a $1/f$-like spectrum, sets the lower limit on the detectable signal level, can be up-converted to higher frequencies corrupting spectra purity (phase noise), and hence is a key design constraint in nearly all analog ICs and systems. Radiation experiments have proven to be very useful in probing the physical noise sources in *npn* SiGe HBTs [3][4].

In this work, we present the first radiation results of complementary SiGe HBTs, and use radiation to probe the differences in underlying physics of 1/f noise between *npn* and *pnp* SiGe HBTs.

II. Device Technology and Experiment

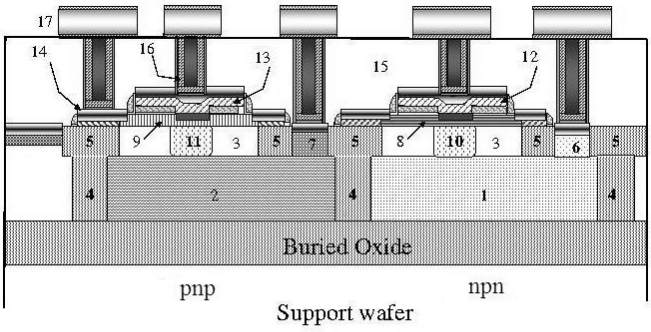

1 N-buried layer (NBL)	6 N-sinker	11 PSIC	16 Contact plug
2 P-buried layer (PBL)	7 P-sinker	12 NEMIT POLY	17 First metal
3 Collector epitaxy	8 NPN SiGe base	13 PEMIT POLY	2^{nd} , 3^{rd} metals not shown
4 Deep trench (DT)	9 PNP SiGe base	14 Silicide	
5 Shallow trench (STI)	10 NSIC	15 BPSG	

Fig. 1. Schematic device cross-section of novel complementary SiGe HBT technology.

This novel complementary SiGe HBT BiCMOS technology (Figure 1) was fabricated by Texas Instruments, and involves dual depositions of SiGe epitaxy (boron doped for the *npn*, and arsenic doped for the *pnp*), shallow and deep trench isolation, polysilicon emitter contacts with thin, interfacial oxide layers (more process details can be found in [2]). Both *npn* and *pnp* SiGe HBTs, as well as the Si CMOS devices, were integrated on SOI material. In addition, both *pnp* and *npn* devices have been optimized with separate emitter processes in the standard process to reach f_T=28GHz. Due to the need of achieving comparable current gain between the *npn* and *pnp* transistors, a controlled emitter interfacial oxide (between the single crystal Si emitter and the heavily doped polysilicon contact) was used to independently adjust the *npn* and *pnp* transistors. Because such interfacial oxides are known to affect low-frequency noise, we have also compared two complementary SiGe HBT processes fabricated

identically, except with differing interfacial oxide thicknesses on the *npn* SiGe HBT (the *pnp* emitter process was held fixed).

Transistors of varying geometries were measured. The width of both the *npn* and *pnp* devices was fixed at 0.4μm, while the length was varied from 0.8μm to 6.4μm. Measured pre-radiation cutoff frequencies (f_T) of the complementary SiGe HBTs are both 19 GHz, with Early voltages (V_A) of the *npn* and *pnp* transistors of 150V and 100V, respectively [2]. The samples were irradiated with 63.3 MeV protons at the Crocker Nuclear Laboratory at the University of California at Davis. Experiments with proton fluxes from 10^6 to 10^{11} $p/cm^2/s$ can be achieved in the beam current range from about $5pA$ to $50nA$. The details of the dosimetry system , which has accuracy up to about 10%, are described in [5] and [6]. At proton fluences of 1.0×10^{12} and 5.0×10^{13}p/cm^2, the measured equivalent gamma dose was approximately 135 and 6,759 krad(Si), respectively.

An automatic noise measurement was developed to measure the noise power spectral densities of the devices. The block diagram of the system is shown in Figure 2.

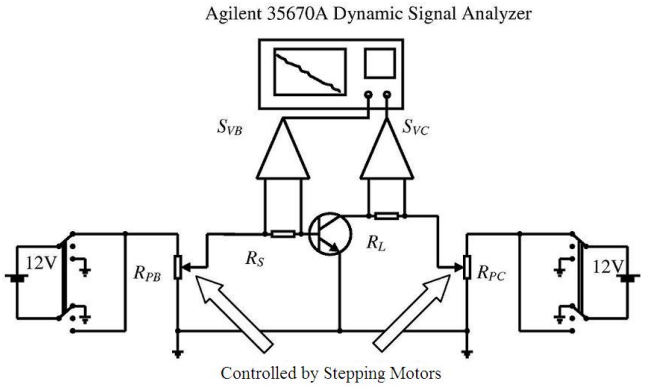

Fig. 2. Schematic block diagram for the automatic dual-channel noise measurement system.

Wire-wound potentiometers R_{PB} and R_{PC} are controlled by a computer through two stepping motors. Since the control system between the stepping motors and the computer is isolated by relays, the 60Hz fluctuations from the ac power source do not degrade the measured data. An Agilent 35670A Dynamic Signal Analyzer was used to measure the voltage power spectrum densities S_{VB} and S_{VC} from resistors R_S and R_L, which are series-connected with the base and the collector terminals, respectively. Typical measured S_{VB} and S_{VC} data are shown in Figure 3. The coherence between those two power spectral densities is found to be close to unity (Figure 4), indicating that the base current noise dominates the device [7].

According to the equivalent hybrid-π model [8], S_{VB} and S_{VC} are given by:

$$S_{VB} \approx (\frac{R_S r_\pi}{R_S + r_\pi})^2 S_{IB} \quad (1)$$

$$S_{VC} \approx (\frac{R_L R_S \beta}{R_S + r_\pi})^2 S_{IB} \quad (2)$$

where, the dynamic current gain $\beta = dI_C/dI_B$; the dynamic

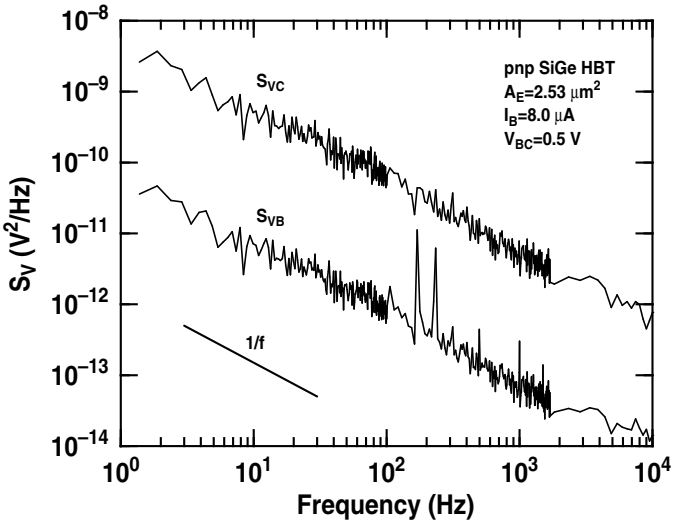

Fig. 3. Typical power spectral densities S_{VB} and S_{VC} measured from the dual-channel system.

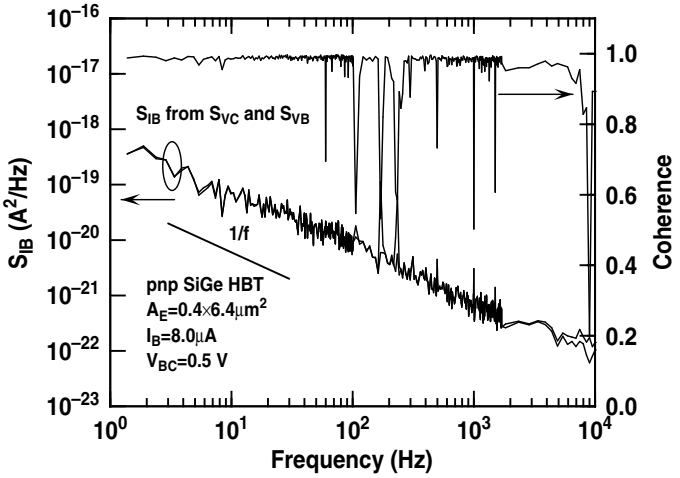

Fig. 4. Extracted power spectral densities S_{IB} from S_{VB} and S_{VC} and measured coherence data.

emitter-base input impedance $r_\pi = dV_{BE}/dI_B$; S_{IB} is the dominant current noise generator in the base. A $1M\Omega$ metal film resistor is chosen for R_S to avoid the parasitic effects from the internal base and emitter resistance and the resistance from the biasing circuits [9]. As shown in Figure 4, S_{IB} extracted from S_{VB} and S_{VC} are very close to each other, which proves that S_{IB} is the dominant noise source.

III. Results

Figure 5 shows the radiation response of the Gummel characteristics for both device types as a function of proton fluence. With increasing fluence, the non-ideal base current component increases, as expected, indicating that radiation-induced G/R traps are being added to the device as the proton fluence increases. Figures 6- 8 show the current gain, and normalized base current change for both *npn* and *pnp* SiGe HBTs in both forward and inverse mode (emitter-base base terminals swapped) as a function of proton fluence. Interestingly, the *pnp* SiGe HBTs generally show significantly better radiation tolerance than the

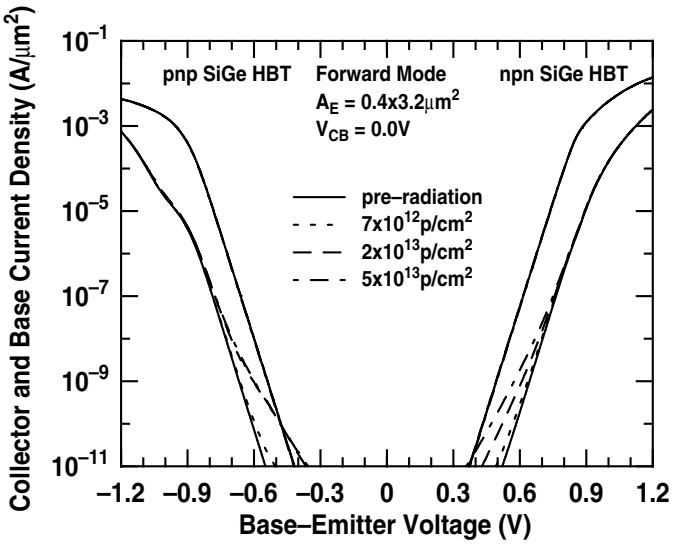

Fig. 5. Gummel characteristics for pre- and post-irradiated complementary SiGe HBTs.

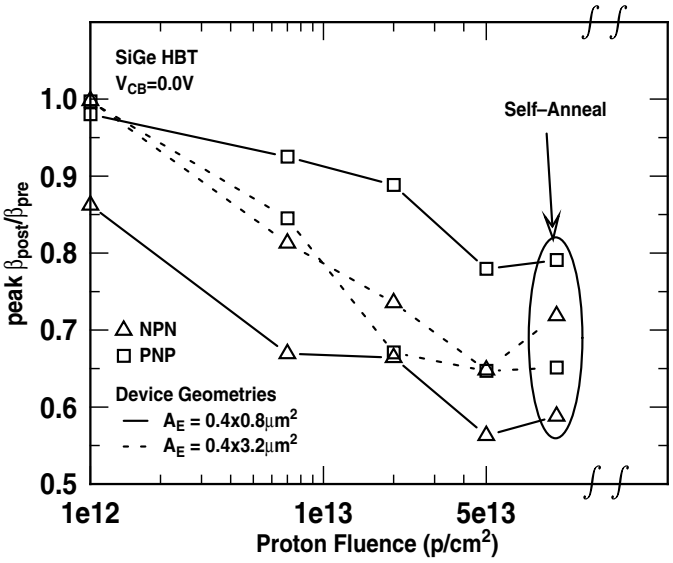

Fig. 6. Current gain degradation for the complementary SiGe HBTs.

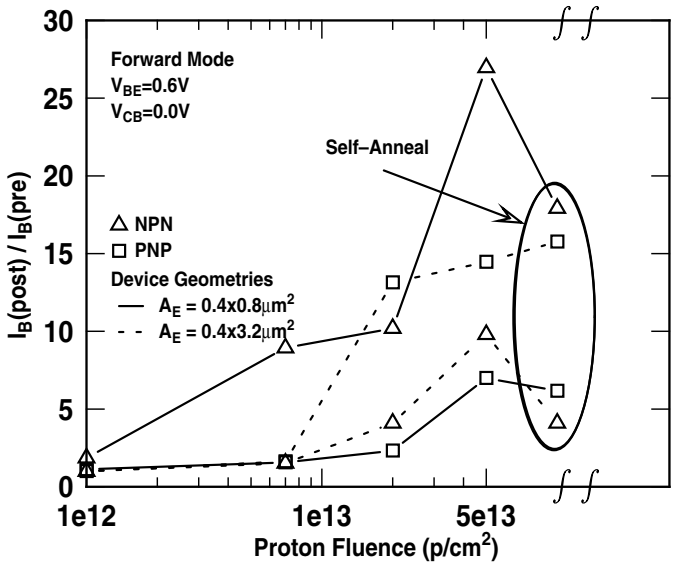

Fig. 7. Base current degradation as a function of fluence in forward mode for the complementary SiGe HBTs.

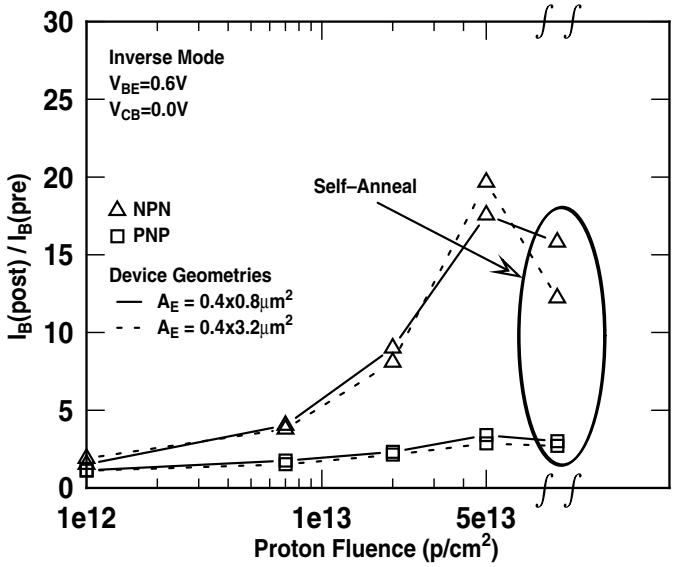

Fig. 8. Base current degradation as a function of fluence in inverse mode for the complementary SiGe HBTs.

npn SiGe HBTs, particularly in inverse mode, although clearly there is a strong dependence on device geometry. This suggests that the damage thresholds between the two device types are fundamentally different, despite the near-identical processing associated with the sensitive damage regions (i.e., the emitter-base spacer oxide and the shallow trench edge). We also consistently observed significant spontaneous self-annealing at room temperature over a span of about 6 weeks.

For the pre-irradiated devices, the noise spectrum is 1/f type in shape and is generally similar to that observed in conventional Si BJTs [9](Figure 9) with the equivalent current noise source S_{IB} exhibiting an I_B^2 dependence and inverse proportionality to emitter area A_E (Figure 10).

We scanned the noise in the devices from $I_B = 0.1\mu$A to $I_B = 8\mu$A. As shown in Figure 9, all of the spectra show a clear 1/f dependences over this base current range and increase with base current I_B. This is also the case for all of the *npn* transistors. To avoid small size effects [10], we focused our studies here on the largest device with A_E=$0.4 \times 6.4\mu$m^2. For the pre-radiation case, The *npn* transistor noise is consistently smaller than that of the *pnp*'s (Figure 11 and Figure 12).

Interestingly, the post-irradiated devices demonstrate a very different behavior for the *npn* and *pnp* SiGe HBTs, as shown in Figure 11 and Figure 12. For the *pnp* transistors, the 1/f noise remains nearly unchanged up to proton fluence of 5.0×10^{13}p/cm^2. For the *npn* transistors, however, the magnitude of the 1/f noise significantly increases after irradiation. This difference in noise response to radiation occurs in spite of the similar response between the *npn* and *pnp* device current-voltage characteristics at the same proton fluence. Even more surprising, in the *npn* SiGe HBTs, at low base currents (I_B<0.8μA) the quadratic dependence of the noise changes to a near linear dependence on base

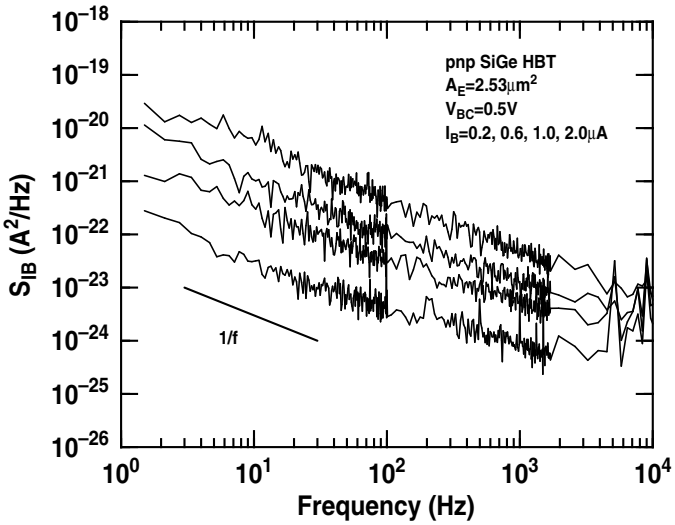

Fig. 9. Extracted power spectral densities S_{IB} at different base currents.

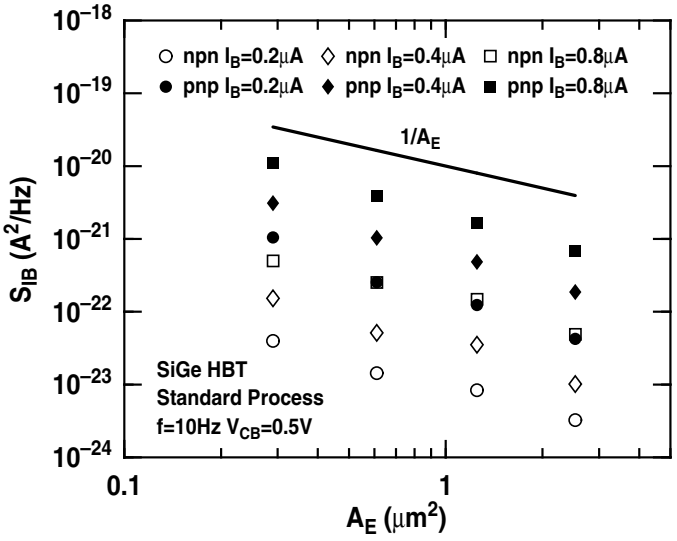

Fig. 10. Extracted power spectra densities S_{IB} at 10Hz as a function of the emitter area.

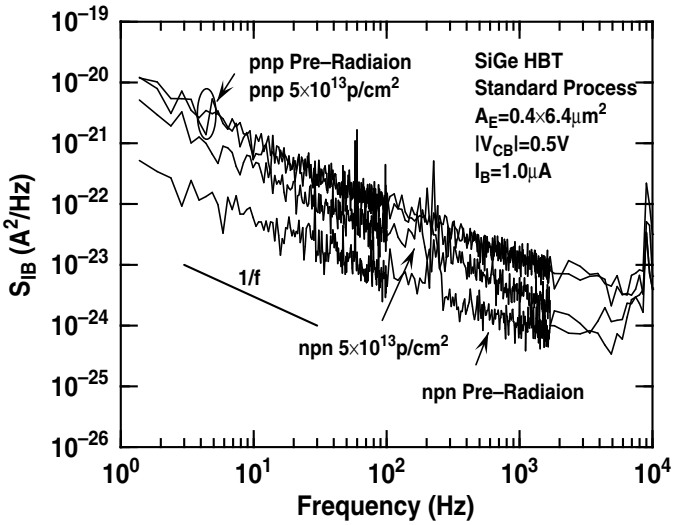

Fig. 11. Comparison of the pre-radiation and the post-radiation S_{IB} spectra for both *npn* and *pnp* SiGe HBTs.

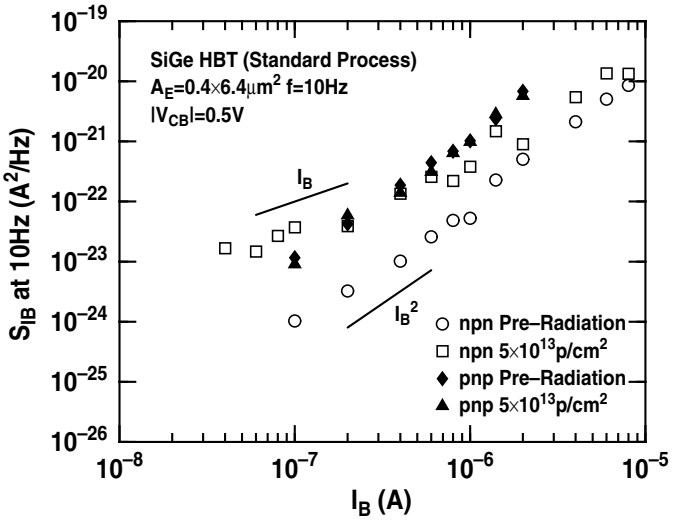

Fig. 12. Effects of irradiation on the bias dependence of the noise at 10Hz for both *npn* and *pnp* SiGe HBTs.

current after radiation exposure, remaining as an I_B^2 dependence at higher bias levels. No such behavior is seen in the *pnp* transistors.

S_{IB} at 10 Hz comparison for the devices with the different *npn* interfacial oxide are shown in Figure 13. As expected, the *npn* SiGe HBT with the thicker interfacial oxide has a larger 1/f noise magnitude, indicating the low frequency noise is mainly caused by the interfacial oxide before irradiation exposure. Note, however, that the *npn* device with the thicker interfacial oxide also exhibits the same anomalous I_B dependence at low base currents as seen in the standard process, suggesting that the observed differences in noise physics between the *npn* and *pnp* SiGe HBTs is fundamental, and not dependent on differences in the emitter interface preparation.

IV. Theory and Discussion

The "tunneling-assisted trapping" model predicts a *linear* dependence of S_{IB} on the base current I_B [11][7]. This model assumes that the 1/f noise results from the dynamic carrier trapping and detrapping processes when carriers are close to the spacer oxide covering the emitter-base junction. The surface recombination base current I_S (in an *npn* transistor) has an exponential dependence on the surface potential ψ_S at the emitter-base space charge region, shown in Figure 14, as $I_S \propto exp(q\psi_S/kT)$, while the surface potential can be modulated by the change in the surface charge Q_S at the $Si-SiO_2$ interface. Therefore, the departure from the pre-radiation surface potential is given by:

$$\triangle\psi_S = \frac{\triangle Q_S}{A_S C_S} \tag{3}$$

with A_S being the effective surface area of the space charge region and C_S the effective surface capacitance per unit area. The fluctuation of the surface recombination current, consequently, can be expressed as:

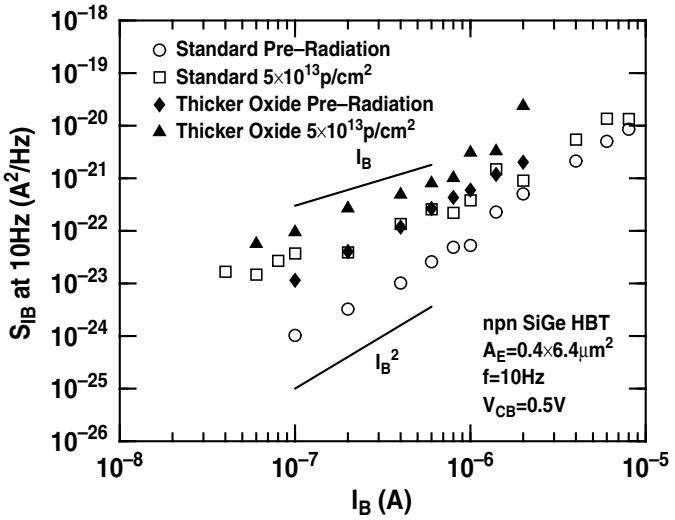

Fig. 13. Effects of irradiation on the bias dependence of the noise at 10Hz in *npn* SiGe HBTs with different interfacial oxide thicknesses.

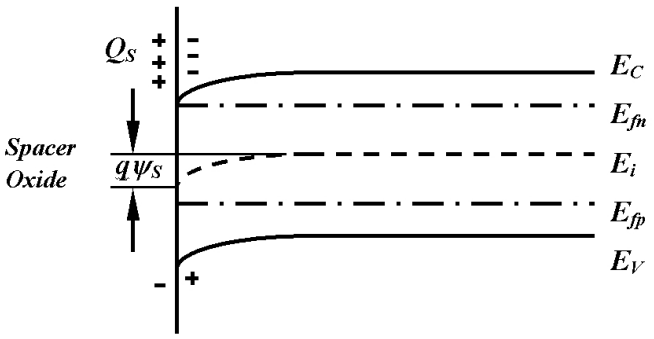

Fig. 14. Cross section of emitter-base space charge region at the spacer oxide edge.

$$\frac{\triangle I_S}{I_S} = \frac{\partial ln(I_S)}{\partial \psi_S}\triangle\psi_S = \frac{q}{kT}\cdot\frac{\triangle Q_S}{A_S C_S} \tag{4}$$

Thus, the power spectral density of the surface recombination current fluctuation S_{IS} becomes:

$$S_{IS} = \frac{q^2}{k^2T^2}\cdot\frac{S_{QS}}{A_S C_S^2} I_S^2 \tag{5}$$

where S_{QS} is the surface charge spectral density per unit area. The surface charge fluctuation originates from the trapping-detrapping of carriers between the slow states inside the spacer oxide and the space charge region through the tunneling process. Assuming only the traps close to the carrier quasi-Fermi level contribute to fluctuations and the trap density is nearly uniform in space, the spectral density S_{QS} in the element tunneling depth $\triangle z$ is [12]:

$$\triangle S_{QS} = 4kTq^2N_t\frac{\tau(z)}{1+\omega^2\tau^2(z)}\triangle z \tag{6}$$

with N_t being the trap density in units of $(cm^{-3}\cdot eV^{-1})$ and $\tau(z)$ the trapping time constant for a slow state trap at position z, which is given by:

$$\tau(z) = \tau_S\cdot exp(z/\lambda) \tag{7}$$

with τ_S the mean time constant and λ the effective attenuation tunneling distance. Substituting Eq.(7) into Eq.(6), the entire oxide charge spectral density S_{QS} is expressed by:

$$S_{QS} = \int 4kTq^2N_t\frac{\tau(z)}{1+\omega^2\tau^2(z)}dz = 4kTq^2N_t\lambda\frac{\pi/2 - tan^{-1}(\omega\tau_s)}{\omega} \tag{8}$$

Since τs is on the order of μs, $tan^{-1}(\omega\tau_s)$ is negligible up to $f = 100KHz$. Therefore, S_{QS} becomes:

$$S_{QS} \approx kTq^2N_t\lambda/f \tag{9}$$

Substituting Eq.(9) into Eq.(5) and assuming the surface recombination fluctuation is the dominant noise source ($S_{IB} \approx S_{IS}$), S_{IB} can be expressed as:

$$S_{IB} = \frac{q^4N_T\lambda}{kTA_SC_S^2f}I_S^2 \tag{10}$$

Since the base current I_B is composed of a diffusion current and the surface recombination current, it can be defined by:

$$I_B = I_D + I_S \approx I_{B0}\cdot exp(qV_{BE}/kT) + I_{S0}\cdot exp(qV_{BE}/2kT) \tag{11}$$

where I_D is the diffusion current, and I_{B0} and I_{S0} are the diffusion and surface saturation currents, respectively. Therefore, the base current fluctuations can be expressed as:

$$S_{IB} = \frac{q^4N_T\lambda}{kTA_SC_S^2f}\frac{I_{S0}^2}{I_{B0}}I_B \tag{12}$$

This noise model predicts that S_{IB} is inversely proportional to emitter periphery (P_E), since the surface area of the emitter-base space charge region A_S is proportional to the emitter periphery. As can be seen in Figure 15, the pre-irradiated devices exhibit a clear $1/A_E$ dependence, while the post-irradiated transistors deviate from this behavior. More noise data on devices with differing P/A ratios will be required to clearly differentiate if this follows a $1/P_E$ behavior, and is in progress.

The carrier number fluctuations in the diffusion component of the base current are much more complicated than that in the surface recombination component. Several noise models associated with different physical mechanisms, which predict an I_B^2 dependence of S_{IB}, have been reported in [13]-[16]. The "transparency fluctuation model" proposed by Kleinpenning assumes that the thermal noise from the interfacial oxide can modulate the oxide barrier height. Hence, the oxide generates the so-called "transparency fluctuation," or tunneling probability fluctuation, through the oxide [13]-[15]. Thus, the current passing through the emitter is modulated by the transparency fluctuation, which

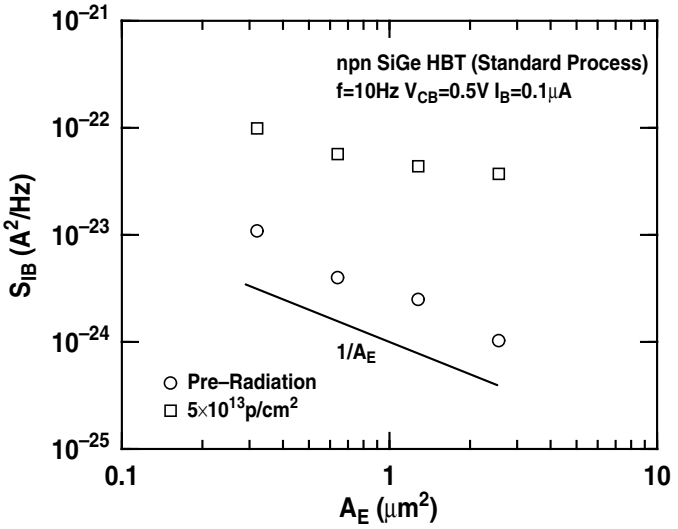

Fig. 15. Effects of irradiation on the geometrical dependence of hte *npn* and *pnp* SiGe HBTs.

induces 1/f noise. This model predicts that the 1/f noise has a cubic dependence on the interfacial oxide thickness.

Another noise model worth mentioning is the "two-step tunneling model", used to explain the low frequency noise in tunnel diodes [16]. For the first step, the carriers recombine with the bound states at the $Si - SiO_2$ interface close to the monosilicon region. Then, some of the carriers are trapped by the slow states inside the oxide through tunneling process in the second step. This model, eventually, predicts a quadratic dependence of 1/f noise on the interfacial oxide thickness.

However, these models are not suitable to explain the exponential dependence of 1/f noise on the interfacial oxide thickness found in our experiments. A possible physical mechanism for this strong oxide thickness dependence is that the 1/f noise comes from the trapping-detrapping process associated with the slow states inside the interfacial oxide. The approximate exponential energy distribution of the trap density, finally, leads to the exponential dependence of low frequency noise on the interfacial oxide thickness.

From all of these experiments, we consistently find that the magnitude of the 1/f noise of *pnp* transistors is larger than for the *npn* transistors within the same fabrication process, except for the *npn*'s 1/f noise associated with the surface recombination current. The difference between the 1/f noise of *npn* and *pnp* transistors is believed due to the different properties of electron and hole traps in the composite material used in the interfacial oxide. In our case, the hole trap density in *pnp* transistor is believed to be several orders of magnitude higher than the electron trap density in the *npn*, as other authors have reported [17]. Hence, the additional trap density induced by irradiation might in fact be comparable for both the *npn* and *pnp* devices, but still negligible compared to the pre-radiation density found in the *pnp* devices, thus producing only an apparent higher radiation tolerance for the *pnp* SiGe HBT compared to the *npn* SiGe HBT. More work will be needed to definitively answer this.

V. Summary

This work presents the first radiation results on complementary SiGe HBTs, and uses radiation to probe the differences in underlying physics of 1/f noise between *npn* and *pnp* SiGe HBTs. For pre-irradiation *npn* and *pnp* transistors, both types show 1/f type of low frequency noise spectrum, quadratic dependence on the base current, and inverse proportionality on the emitter area, similar to the conventional complementary Si BJTs. The dominant low frequency noise source is found to be in the interfacial oxide layer between the monosilicon emitter and the polysilicon emitter. For post-radiation *pnp* transistors with radiation dose up to 5.0×10^{13}p/cm^2, the 1/f noise remains unchanged, indicating negligible hole trap centers have been added. However, the magnitude of the 1/f noise for the *npn* transistor increases significantly after irradiated with the same dose, as a result of an increased electron trap density. Additional traps induced by the radiation are added into both the interfacial oxide and the emitter-base spacer oxide. At low base currents ($I_B < 0.8\mu A$), the 1/f noise is dominated by the fluctuation of the surface recombination current, while at the high base currents, the 1/f noise is still caused by the traps inside the interfacial oxide.

VI. Acknowledgement

The authors would like to thank Z. Jin, J. Lee, L. Cohn, K. LaBel, and TI BiCOM3 SiGe team for their contributions to this work.

References

[1] J. D. Cressler and G. Niu, *Silicon-Germanium Heterojunction Bipolar Transistors,* Artech House, 2003.

[2] B. El-Kareh, S. Balster, W. Leitz, P. Steinmann, H. Yasuda, M. Corsi, K. Dawoodi, C. Dirnecker, P. Foglietti, A. Haeusler, P. Menz, M. Ramin, T. Scharnagl, M. Schiekofer, M. Schober, U. Schulz, L. Swanson, D. Tatman, M. Waitschull, J. W. Weijtmans, and C. Willis, "A 5V complementary-SiGe BiCMOS technology for high-speed precision analog circuits," *Proc. IEEE BCTM*, pp. 211-214, 2003.

[3] Z. Jin, J. D. Cressler, G. Niu, P. W. Marshall, H. S. Kim, R. Reed, and A. J. Joseph, "Proton response of low-frequency noise in 0.20μm 90 GHz f_T UHV/CVD SiGe HBTs," *Solid-State Elec.*, vol. 47, pp. 39-44, 2003.

[4] Z. Jin, G. Niu, J. D. Cressler, C. J. Marshall, P. W. Marshall, H. S. Kim, R. A. Reed, and D. L. Harame, "1/f noise in proton-irradiated SiGe HBTs," *IEEE Trans. Nucl. Sci.*, vol. 48, pp. 2244-2249, 2001.

[5] P. W. Marshall, C. J. Dale, M. A. Carts, and K. A. LaBel, "Particle induced bit errors in high performance fiber optic data links for satellite data managment," *IEEE Trans. Nucl. Sci.*, vol. 41, pp. 1958-1965, 1994.

[6] K. M. Murray, W. J. Stapor, and C. Castenada, "Proton beam facility for single event research," *Nucl. Instrum. Methods*, vol. B56/57, p. 616, 1991.

[7] E. Zhao, Z. Celik-Butler, F. Thiel, R. Dutta, "Temperature dependence of 1/f noise in polysilicon-emitter bipolar transistors," *IEEE Trans. Elec. Dev.*, vol. 49, pp. 2230-2236, 2001.

[8] S.P.O. Bruce, L. K. J.Vandamme, and A.Rydberg, "Measurement of low-frequency base and collector current noise and coherence in SiGe heterojunction bipolar transistors using transimpedence amplifiers," *IEEE Trans. Elec. Dev.*, vol. 46, pp. 993-1000, 1999.

[9] M. J. Deen, J.Iiowski, and P.Yang, "Low frequency noise in polysilicon-emitter bipolar junction transistors," *J. Appl. Phys.*, vol. 77, pp. 6278-6288, 1995.

[10] Z. Jin, J. D. Cressler, N. Guofu, A. J. Joseph, "Impact of geometrical scaling on low-frequency noise in SiGe HBTs," *IEEE Trans. Elec. Dev.*, vol. 50, pp. 676-682, 2003.

[11] A. Mounib, G. Ghibaudo, F. Balestra, D. Pogany, A. Chantre, and J. Chroboczek, "Low frequency (1/f) noise model for the base current in polysilicon emitter bipolar junction transistors," *J. Appl. Phys.*, vol. 79, pp. 3330-3336, 1996.

[12] H. Hong, "Low-frequency noise study in electron devices: review and update," *Microelec. Reliability.*, vol. 43, pp. 585-599, 2003.

[13] H. A. W. Markus, and T. G. M. Kleinpenning, "Low-frequency noise in polysilicon emitter bipolar transistors," *IEEE Trans. Elec. Dev.*, vol. 42, pp. 720-727, 1995.
[14] T. G. M. Kleinpenning, "On low-frequency noise in tunnel diodes," *Solid-State Elec.*, vol. 21, pp. 927-931, 1978.
[15] T. G. M. Kleinpenning, "On low-frequency noise in tunnel diodes," *Solid-State Elec.*, vol. 25, pp. 78-79, 1982.
[16] V. Kumar, and W. E. Dahlke, "Low frequency noise in $Cr - SiO_2 - n - Si$ tunnel doides," *IEEE Trans. Elec. Dev.*, vol. 24, pp. 146-153, 1977.
[17] H. Miki, M. Noguchi, K. Yokogawa, K. Bo-Woo, K. Asada, and T. Sugano, "Electron and hole traps in SiO_2 films thermally grown on Si substrates in ultra-dry oxygen," *IEEE Trans. Elec. Dev.*, vol. 35, pp. 2245-2252, 1988.